Astrophysics, Vol. 54, No. 1, March, 2011

ATOMIC LINE BROADENING BY THERMAL ENERGY FLUCTUATIONS IN STELLAR ATMOSPHERES AND PLASMA DIAGNOSTICS

O. Cardona

A new method for finding the line widths of atomic lines produced by thermal energy fluctuations in a gaseous system is developed assuming that the atomic linear density change in the energy of the levels is equal to the linear density of the energy fluctuations per degree of freedom. A formula is derived for the atomic line widths that depends on temperature, the cubic root of the total number density of particles in the system, and on the sum of the squares of the principal quantum numbers of the states that participate in the transitions that produce the lines. The calculated widths agree well with the published experimental and theoretical values. This formula will be useful for directly diagnosing the physical state of stellar atmospheres and plasmas.

Key words: *atomic processes:line:profiles - stars:atmospheres*

1. Introduction

The spectroscopic emission lines of the chemical elements produced by stellar atmospheres and plasmas show a characteristic intensity profile as a function of frequency with a central maximum that decrease away from this maximum. The width of this profile is an important measurable parameter for the diagnostics of the physical state of plasmas. The profile of the atomic lines in plasmas directly contains information on the physical conditions of the gas under study. The line profiles depend upon the local density and temperature of the medium. Therefore, the line profiles provide a valuable experimental and theoretical diagnostic tool. There are several physical processes that produce a fuzziness of the atomic lines in a plasma, the line broadening. For an isolated atom, the spectral lines are nearly perfectly sharp. The finite lifetime of the atomic levels due to radiative decay will itself naturally broaden the lines. Natural broadening takes place even for isolated atoms. In a plasma one observes an ensemble of atoms moving

Instituto Nacional de Astrofísica, Óptica y Electr´onica, México; e-mail: ocardona@inaoep.mx

Published in Astrofizika, Vol. 54, No. 1, pp. 89-101 (February 2011). Original article submitted September 3, 2010.

with a velocity distribution along the line of sight, and the profile seen from the entire ensemble is a superposition of these Doppler-shifted atomic profiles. In a plasma there would be additional broadening of the lines, called pressure broadening, caused by perturbations of the wave-train radiated by the atoms through collisions with other atoms and charged particles in the gas. Pressure broadening is described by two approximate theories. One is the impact theory where the radiating atom is an oscillator that suffers an instantaneous collision that interrupts the radiation wave train with a sudden phase shift, or by inducing a transition. These collisions thus cause a finite duration of emission of the radiation that introduces a frequency spread in the radiated wave train, and a shift of the line away from its unperturbed frequency. The other is the statistical theory in which the atom is radiating in an electric field produced by an ensemble of particles. This field will fluctuate statistically about some mean value as a result of motions of the particles and produces shifts that alter the frequency of the line. The quantum theory of pressure broadening takes into account the structure of the atoms and yields profiles and shifts in good agreement with experimental determinations. The quantum theory has become very refined and several treatises exist on the general subject of line broadening [1-5]. The theories of pressure line broadening mentioned above are based on local inter-particle physical interactions and their generalizations, to try to take into account the whole ensemble of particles in the system.

On the other hand, in a perfect gas the only interactions that an atom can have with the other particles of the gas is through collisions and thermal energy fluctuations. The collisions are taken into account in the theories presented before. The thermal energy fluctuations in a perfect gas in thermodynamic equilibrium are another physical process for broadening the atomic lines. A new method for finding the width of the atomic lines using the thermal energy fluctuations is presented in this work assuming that the perturbations of the levels are produced by these fluctuations. This is a thermodynamic and statistical mechanics approach for treating the line broadening similar to the methods used for finding the atomic partition function [6] and the widths of the hydrogenic lines [7]. Thermal energy fluctuations are a global collective phenomena by nature.

In what follows, Section 2 introduces the results of statistical mechanics of the energy fluctuations that are used in the development of the model. The model is introduced in Section 3 for hydrogen atoms, and in subsections 3.1 and 3.2 for other atoms and ions. In Section 4 a comparison of the experimental determinations of the line widths with the results of the model is made. Finally, in Section 5 some conclusions are presented.

2. Fluctuations

The physical quantities that describe a macroscopic thermodynamic system in equilibrium are very nearly equal to their mean values. Nevertheless, deviations or fluctuations from the mean values, though small, do occur, and it is essential to use the probability distribution of these deviations. The probability of fluctuations of the thermodynamic variables in a system, using the entropy, is given by [8]

$$P(\Delta S) = Q \exp\left(\frac{\Delta S}{k}\right), \tag{1}$$

where ΔS is the entropy production associated with a fluctuation that takes the system away from the equilibrium state, Q is a normalization constant introduced to make the sum of the probabilities over the possible fluctuations unity, and k is the Boltzmann constant. Expressing ΔS in terms of other thermodynamic quantities and expanding around the equilibrium values gives the mean square fluctuations of various physical quantities [9,10]. For example, the mean square fluctuation of the energy, σ^2, is given by

$$\sigma^2 = \frac{\tau^2}{C_V}, \tag{2}$$

where C_V is the specific heat at constant volume and τ is the mean energy. One can derive the mean square fluctuation in energy of a system of fixed volume in thermal contact with a reservoir using the partition function to relate the change in energy with respect to temperature to the mean square fluctuations given by [11]

$$\sigma^2 = \tau^2 \left(\frac{\partial U}{\partial \tau} \right)_V, \tag{3}$$

where σ^2 is the variance and U is the mean energy of the thermodynamic system and is equivalent to Eq. (1). The full width at half maximum (FWHM) for the distribution of the fluctuations is given by $\gamma = 2\sqrt{2\ln 2}\sigma$. Equation (3) is the fundamental expression for developing the model in the following section.

3. Model

The basic idea of the model is relating the atomic energy of the levels to the energy fluctuations of the system considering that the change in energy of the levels is produced by the fluctuations in energy. The change in energy produced by the perturbations is divided by the size of the orbit of a given atomic state to obtain the linear density of the change that can be compared with the linear density of the fluctuations. The linear density is used because the orbit is changed slightly by the perturbations; therefore, one has to take into account the size of the orbit to distribute those changes during the motion of the electron in the orbit. On the other hand, the thermal energy fluctuations are divided by the size of the box that is available to each atom in the system to obtain the linear density of the fluctuations. The principal assumption in this model is that these two linear energy densities are equal to each other. The model is developed first for hydrogen atoms and later generalized for other atoms and ions.

3.1. Hydrogen Atoms. We start with a thermodynamic system with total number of particles per cubic centimeter N and temperature T in thermodynamic equilibrium, the main variables in stellar atmospheres. The volume occupied by each particle in the gas is taken as cubic and of side L and so is defined by

$$L^3 = \frac{1}{N}. \tag{4}$$

The energy of a hydrogen atom in quantum state n is given by quantum mechanics as

$$E_n = -\frac{RyZ^2}{n^2}, \tag{5}$$

where Ry is the energy of one Rydberg. The change in energy due to a perturbation of a level can be expressed by

$$\delta E_n = \frac{2RyZ^2}{n^3}\delta n. \tag{6}$$

The mean square fluctuation, the variance of a Gaussian distribution, in energy for a systems with constant volume V is given by (Eq. 3),

$$\sigma^2 = \frac{3}{2}(kT)^2, \tag{7}$$

where $U = 3kT/2$, the mean energy of the system, was used in Eq. (3). The mean fractional energy fluctuation per degree of freedom is defined as

$$\Delta = \frac{\sigma^2}{3U} = \frac{kT}{3}. \tag{8}$$

The linear density of the fluctuations is obtained from the following expression:

$$\delta U = \frac{\Delta}{L} = kT\frac{\sqrt[3]{N}}{3}. \tag{9}$$

The linear density change in energy of the level is given by

$$\frac{\delta E_n}{2\pi r_n} = \frac{\alpha RyZ^2}{\pi r_n n^3}\delta n, \tag{10}$$

where r_n is the radius of the orbit with principal quantum number n, and α is a numerical factor that produces the FWHM of the level that has become a Gaussian distribution due to the perturbations produced by the fluctuations. Our principal assumption requires equating Eqs. (9) and (10) to obtain

$$\delta n = \frac{\pi r_n n^3}{3\alpha RyZ^2}kT\sqrt[3]{N}. \tag{11}$$

Substituting Eq. (11) into Eq. (6) gives

$$\delta E_n = \frac{2\pi r_n}{3\alpha} n^2 kT \sqrt[3]{N} \,, \tag{12}$$

for the width of the level n. We now use in Eq. (12) $r_n = a_0 n^2/Z$, the radius of the orbit of the electron, the most probable distance, for the quantum state n for a hydrogen atom derived from quantum mechanics [12,14], where a_0 is the Bohr radius and Z is the atomic number of the atom, to finally obtain

$$\delta E_n = \frac{2\pi a_0 kT \sqrt[3]{N}\, n^2}{3\alpha Z} \,, \tag{13}$$

which represents the width of the level of principal quantum number n. For a line between two levels n_1 and n_2 by convolution of two gaussians the FWHM of the line is [3]

$$w = \frac{2\pi a_0}{3\alpha Z} kT \sqrt[3]{N} \left(n_1^2 + n_2^2\right). \tag{14}$$

This is the main result of the model for the line width at half maximum for hydrogenic atoms in ergs. The convolution of the Gaussian distribution of the fluctuations with the Lorentzian of the natural broadening produces a Voigt profile for the lines, where now α is composed of some numerical factors to obtain the FWHM of the level and of the line times the normalization constant of the Voigt function [13] and is defined by

$$\alpha = \pi\sqrt{\pi}\left(2\sqrt{2\ln 2}\right)^2 \tag{15}$$

3.2. Non-hydrogen atoms. The above results can be generalized to non-hydrogen atoms and ions using the effective charge that the electrons feel and the effective quantum numbers of the levels involved in the transition. The effective charge is obtained considering that the electron making the transition is in a field produced by the screened atomic nucleus by the inner or core electrons. The screening can be taken into account using as the effective charge $Z_{eff} = J + 1$, where J is the ionization state of the chemical element with $J = 0$ for neutral atoms, $J = 1$ for single ionized atoms, etc. The effective quantum numbers are obtained from the tables of experimental and theoretical energy levels of the atoms [15,16] and are expressed by

$$n_{eff} = Z_{eff} \sqrt{\frac{Ry}{E_n}} \,, \tag{16}$$

where E_n is the energy of the level with respect to the continuum in Rydbergs Ry obtained from the tables. Then instead of Eq. (15) one has the expression

$$w = \frac{2\pi a_0}{3\alpha Z_{eff}} kT \sqrt[3]{N} \left(n_{eff\,1}^2 + n_{eff\,2}^2\right) \tag{17}$$

for the full width at half maximum of the line for the non-hydrogen atoms in ergs

4. Comparison with Experimental Results

A comparison between theoretical and experimental line widths is difficult because the experimental line widths are given for temperature and electron densities n_e and sometimes the proportion of the constituents is not given, and Eqs. (14) and (17) depend on the total number density of particles in the given medium. For a gas composed of pure hydrogen, one can obtain the total number density from the expression

$$N = \frac{n_e}{\phi(T)} + 2\,n_e\,, \tag{18}$$

where

$$\phi(T) = \frac{2U_1}{U_0}\left(\frac{2\pi mkT}{h^2}\right)^{3/2} \exp^{-\chi_1/kT}\,, \tag{19}$$

is the Saha factor and the U's are the partition functions of the neutral and ionized hydrogen, h is Planck's constant, and χ_1 is the ionization potential for hydrogen. When the gas is a mixture of different atoms, the composition given by their concentrations or abundances must be known. Given the electron densities and following the normal calculations of the equation of state [3,17], one can obtain the total number density of particles. Equations (14) and (17) are expressed in frequency units (*Hz*), and the results are transformed into wavelength units, angstroms (Å) using

$$\Delta\lambda = \frac{\lambda^2}{c}\Delta\nu\,, \tag{20}$$

where $\Delta\lambda$ and $\Delta\nu$ are the widths in wavelength and in frequency units, respectively, and λ is the wavelength of the given line. For hydrogen lines the calculations are made with pure hydrogen, and for helium, lines with pure helium due to the lack of information on the exact concentrations of the experimental and theoretical mixtures.

The curves in Fig.1 show the width of hydrogen Lyman-α in Å as a function of electron number density for temperatures 10^4, 1.2×10^4, 1.5×10^4, and 2×10^4 K. The asterisks are the experimental FWHM of the hydrogen Lyman-α line emitted from an argon plasma studied in the benchmark experiment by Grützmacher and Wende [18-20] for the different temperatures. The theoretical results [21] are very close to the experimental values and it difficult to distinguish them in the figures. The results of the model for a pure hydrogen plasma are in good agreement with both results for the temperature of 1.27×10^4 K. Figure 2 shows the width of Hα in Å as for Fig. 1 compared with the experimental FWHM of the hydrogen Balmer-α line emitted from argon plasmas studied in benchmark experiments

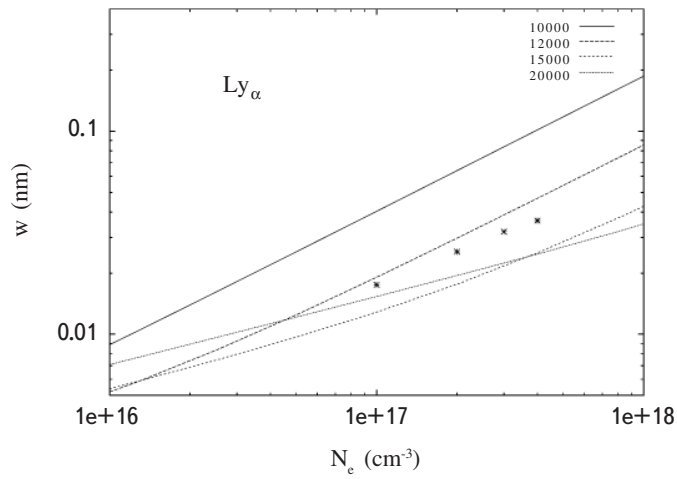

Fig.1. The curves show the width of hydrogen Lyman-α in Å from the model for the temperatures in the right upper corner, compared with the experimental FWHM of the hydrogen Lyman-α line emitted from an argon plasma [18-20] for the different temperatures. The calculated results [21] are very close to the experimental values and it difficult to distinguish them in the figure.

by Wiese et al. [22] and by Vitel [23], and emitted by a helium plasma of the gas-linear pinch studied by Büscher et al. [24]. The asterisks are experimental results for argon, and squares for helium plasmas, for different temperatures. The theoretical values [21] are represented by crosses. The results of the model for pure hydrogen are of the order

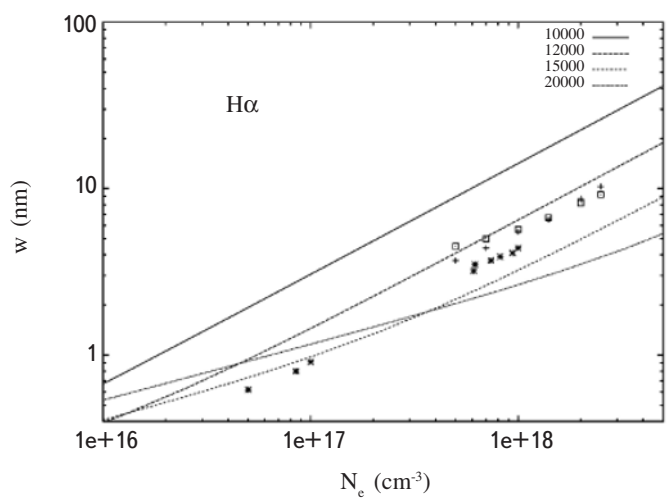

Fig.2. The curves show the width of hydrogen Balmer-α in Å from the model for the temperatures as in Fig.1, compared with the experimental FWHM of the hydrogen Balmer - α line emitted from argon plasmas [22] and by Vitel [23], and emitted by a helium plasma of the gas-linear pinch [24]. The calculated results [21] for argon are very close to the experimental values, and it is difficult to distinguish them in the figure, and the ones for helium are shown by crosses.

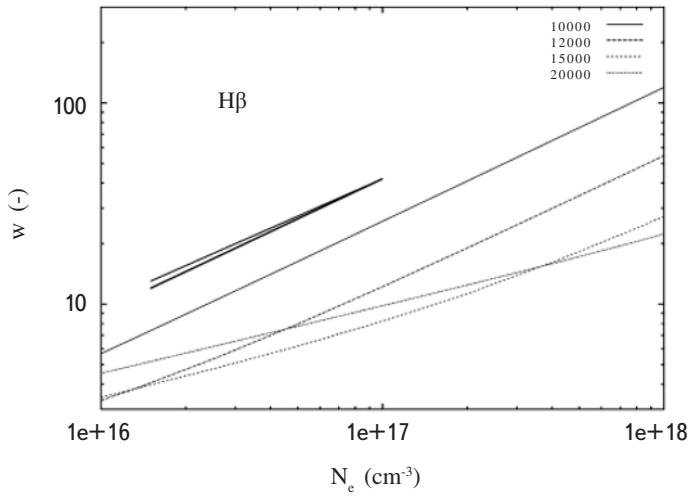

Fig.3. The curves show the width of hydrogen Balmer-β in Å from the model for the temperatures as in Fig.1 compared with the experimental FWHM of the hydrogen Balmer-β from Wiese et al. [22] and from Fig. 18 of Griem [2], shown as a thin straight line. The thick straight lines are the relaxation theory results [25].

of the experimental and theoretical values. But the difference between the asterisks and squares shows that the different concentrations of hydrogen with respect to argon and helium and different experimental set-ups are fundamental for the correct evaluation of the line widths. Figure 3 shows the width of Hβ in Å as in Fig.1 compared

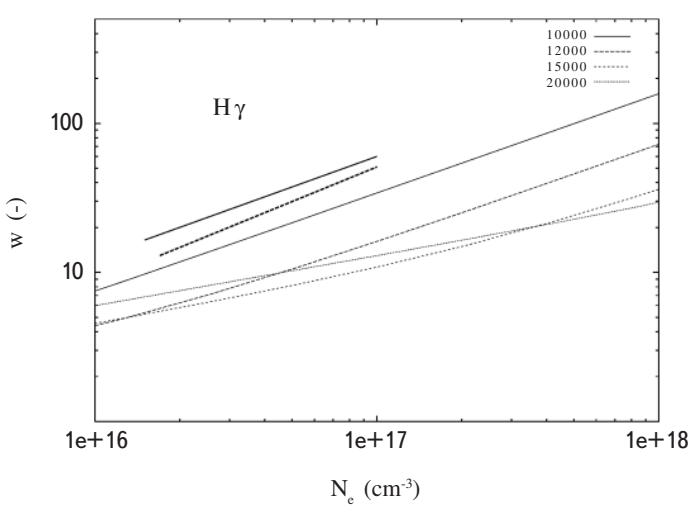

Fig.4. The curves show the width of hydrogen Balmer-γ in Å from the model for the temperatures as in Fig.1, compared with the experimental FWHM from Wiese et al. [22] and from Fig.21 of Griem [2] (thick straight line). The thin straight line are the relaxation theory results [25].

with the experimental FWHM of the hydrogen Balmer-β from Wiese et al. [22] and from Fig.18 of Griem [2], shown as a thin straight line, and the relaxation theory results as a thick straight line [25]. Here again the problems of the concentrations and of the experimental set-ups appear as for the $H\alpha$ line. Therefore, the results are in agreement within the experimental errors. Figure 4 shows the width of $H\gamma$ in Å compared with the experimental FWHM of

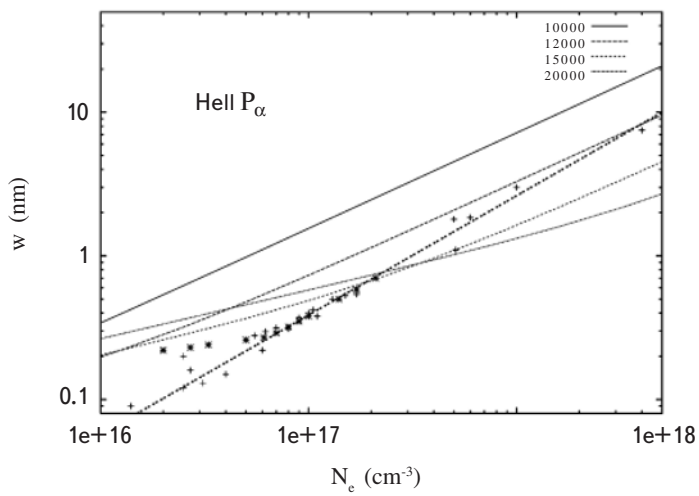

Fig.5. The curves show the width of ionized helium Paschen-α in Å from the model for the temperatures as in Fig.1, compared with experimental widths from different authors (crosses), and with the theoretical calculations of Griem and Shen [27](dash point line). The results of the model for pure helium have a different behavior than the calculations of Griem and Shen [27], represented by the double point line. The experimental values of Pittman and Fleurier [28] shown as asterisks.

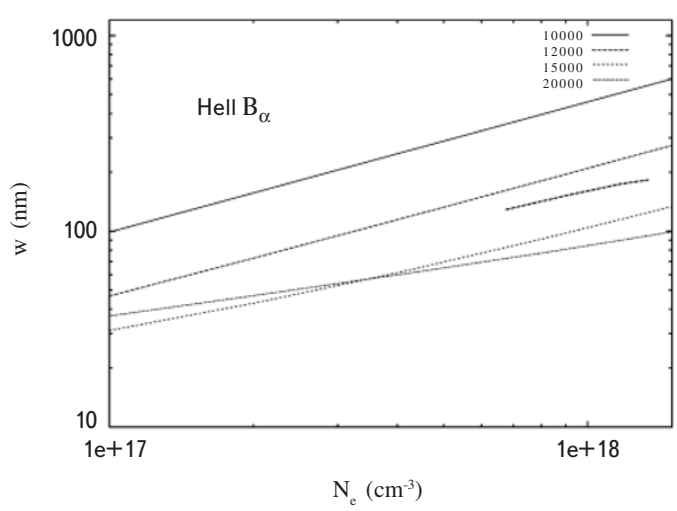

Fig.6. The curves show the width of ionized helium Balmer-α at 1640.7 in pm from the model for the temperatures as in Fig.1, compared with experimental widths [20].

the hydrogen Balmer-γ line from Wiese et al. [22] (straight thick line) and from Fig.21 of Griem [2]. The relaxation theory results [25] are drawn with a thin straight line. The results of the model are similar to those of $H\beta$. Figure 5 shows the FWHM of the He II Paschen-α line measured in different experiments collected in Fig.4.10 of Griem [26] compared with the line widths of He II Paschen-α at 4686 Å as in Fig.1. The results of the model for pure helium have a different behavior than the calculations of Griem and Shen [27], represented by the double point line, and agree with the experimental values for higher densities and with the experimental values of Pittman and Fleurier [28], asterisks, the higher points in the low density regime. Apparently, the collective effects do not cease to exert the perturbations over the levels as could happened in the local theories, producing a greater width of the lines. Figure 6 shows the FWHM of the He II Balmer-α at 1640.7 Å in pm measured in the benchmark experiment by Grützmacher and Johannsen [20]. The results of the calculated values for pure helium are of the order of the experimental and theoretical ones because information over the concentrations of the mixture is absent. The values of the conventional theory by Griem [27] are two times lower than the experimental determinations. The line width of He I ($2p^1P-4d^1D$) at 4922 Å from the line profile measurements by Adler and Piel [29] from Figs.4.7 and 4.8 of Griem [26] and from Fig.7.6 of Fujimoto [5] are in accordance with the calculated values. The line width of C I ($3s^1P-4p^1D$) at 5052 Å measured by Jones and Wiese [30] represented in Fig.4.11 of Griem [26] shows good agreement with the calculated values. The calculated ratio $w(H\gamma)/w(H\beta)$ from formula (14) is 1.32, close to the experimental values and greater than the theoretical values given in Table IV of Griem [2]. The problem of the abundance of the elements in the different experiments make it very difficult to know the contribution of the line broadening by the thermal energy fluctuations to the total broadening of the lines. From the stellar atmospheres point of view, it is difficult to make comparisons with direct observational profiles because one generally cannot measure local values of the plasma emission but must infer them from averages over several contributing volume elements in the stellar atmosphere. Nevertheless, the line widths of some Balmer lines, like H-alpha, beta and gamma for the solar atmosphere [31], are well reproduced by the model using the values given by stellar model atmospheres, with the effective temperature of 5770 K and gravity $g = 3.16\times10^4$ cm/s^2, which give the total number density of particles $N = 10^{16}$ cm^{-3} and a temperature of 4500 K at the region of formation of the lines, for solar abundance of the elements [32].

5. Conclusions

The width of the atomic lines is derived using the linear density of the change in energy of the atomic states and the linear density of the fluctuations in thermal energy per degree of freedom of the gas assuming that these two densities are equal. Another result of the model is that the widths at half maximum of the individual atomic levels are given by Eq. (13). The resulting equations are simple and are functions of the temperature, total number density of particles in the gas, and of the principal quantum numbers of the levels that take part in the transition. The formulas obtained are compared with some experimental line width for the hydrogen atoms and also for some non-hydrogen atoms and ions. The results agree fairly well with the experimental results, taking into account that the results of the model are for pure elements and not for the mixtures used in the different experiments. At high densities the model results are of the order of the experimental determinations of the line widths, and at lower densities the calculated

values are greater than the theoretical values obtained, for example, from Griem and Shen [27] and close to the experimental values of Pittman and Fleurier [28] for the He II Paschen-α line. One can infer from these results that the effects of the global collective ensemble of particles do not stop perturbing the levels of the atoms, even at low densities. Therefore the widths of the lines would be greater than those calculated with other methods and could eliminate the so-called ”microturbulence” effect in stellar atmospheres. The so-called microturbulence in the stellar atmospheres context is introduced when the ob- servational width of the lines does not conform with a predicted theoretical value with a given theory in the curve of growth analysis in stellar atmospheres. To explain this difference, it has been customary to postulate the existence of additional nonthermal motions of the stellar material, which are usually referred to as microturbulence [3]. An extra term is introduced in the definition of the most probable speed for the temperature of the medium under study

$$\xi_0 = \left[\frac{2kT}{Am_H} + \xi_t^2 \right]^{1/2}. \tag{21}$$

This fudge factor ξ_t does not have anything to do with any real physical phenomena. This factor is used in the calculation of model atmospheres as a free parameter. This works shows that one does not need that factor to explain the width of the lines in the low density regime as in the case of stellar atmospheres. The treatment in the article differs completely from the other mechanisms presented in the different theories because it is a global interaction and not a local one as in the other theories. The experimental results do not permit one to discriminate between the different theories. In all the works the Natural and Doppler broadening are taken into account, but the values are small and do not changes the results very much. The model of the line widths with only thermal energy fluctuations explains the gross characteristics of the broadening of the lines. It would be necessary to have better experimental and observational results to study the contribution of this type of line broadening to the general broadening of the lines in stellar atmospheres and plasmas.

The author acknowledges the technical support of María de los Ángeles López Castillo.

REFERENCES

1. H. R. Griem, Plasma Spectroscopy, New York, McGraw-Hill, 1964.
2. H. R. Griem, Spectral Line Broadening by Plasmas, New York, Academic Press, 1974.
3. D. Mihalas, Stellar Atmospheres, San Francisco, Freeman, 1978.
4. I. I. Sobelman, L. A. Vainshtein, and E. A. Yukov, Excitation of Atoms and Broadening of Spectral Lines, Berlin, Springer-Verlag, 1981.
5. T. Fujimoto, Plasma Spectroscopy, Oxford, Claredon Press, 2004.
6. O. Cardona, E. Simonneau, and L. Crivellari, Rev. Mex. Fis., **51**, 476, 2005.
7. O. Cardona, Recent Directions in Astrophysical Quantitative Spectroscopy and Radiation Hydrodynamics, ed I. Hubeny, J. M. Stone, K. MacGregor, and K. Werner, New York, AIP Proceedings, 1171, 2009, p.349.
8. A. Einstein and Jb. Radioakt., **4**, 411, 1907.

9. L. D. Landau and E. M. Lifshitz, Statistical Physics, Oxford, Pergamon Press, 1980.
10. R. K. Pathria, Statistical Mechanics, Oxford, Pergamon Press, 1972.
11. C. Kittel and H. Kroemer, Thermal Physics, New York, W.H.Freeman, 1980.
12. B. H. Bransden and C. J. Joachain, Physics of Atoms and Molecules, Harlow, Prentice-Hall, 2003, p.162.
13. A. Unsöld, Physik der Sternatmosphären (Berlin: Springer-Verlag), 1955.
14. R. B. Leighton, Principles of Modern Physics, New York, McGraw-Hill, 1959, p.180.
15. NIST, 2010, Data http://www.physics.nist.gov/PhysRefData/Handbook/Tables
16. TOP, 2010, http://cdsweb.u-strasbg.fr/topbase/topbase.html
17. O. Cardona, E. Simonneau, and L. Crivellari, Astrophys. J., **695**, 85, 2009.
18. K. Grützmacher and B. Wende, Phys. Rev., **A11**, 1854, 1975.
19. K. Grützmacher and B. Wende, Spectral Line Shapes v.4, Ontario, Windsor, 1978, p.49.
20. K. Grützmacher and U. Johannsen, Spectral Line Shapes v.7, ed R. Stamm and B. Talin, New York, Nova Science Publishers, 1993, p.139.
21. M. A. Gigosos and V. Cardenosos, J. Phys., **B29**, 4795, 1996
22. W. L. Wiese, D. E. Kelleher, and D. R. Paguette, Phys. Rev., **A6**, 1132, 1972.
23. Y. Vitel and J. Phys., **B20**, 2327, 1987.
24. S. Büscher, Th. Wrubel, S. Ferri, and H. -J. Kunze, J. Phys., **B35**, 2889, 2002.
25. C. R. Vidal, J. Cooper, and E. W. Smith, Astrophys. J. Suppl. Ser., **25**, 37, 1973.
26. H. R. Griem, Principles of Plasma Spectroscopy, Cambridge. Cambridge Univ. Press, 1997.
27. H. R. Griem and K. Y. Shen, Phys. Rev., **122**, 1490, 1961.
28. T. L. Pittman and C. Fleurier, Phys. Rev., **A33**, 1291, 1986.
29. H. G. Adler, A. Piel, and J. Quant. Spectrosc. Radiat. Transfer, **45**, 11, 1991.
30. D. W. Jones and W. L. Wiese, Phys. Rev., **A30**, 2602, 1984.
31. R. L. Kurucz, I. Furenlid, J. Brault, and L. Testerman, Solar Flux Atlas From 296 to 1300 nm, National Solar Observatory Atlas NO. 1, Cambridge, Harvard University, 1984.
32. O. Cardona, E. Simonneau, and L. Crivellari, Astrophys. J., **690**, 1378, 2009.